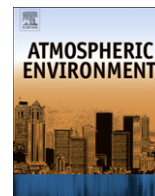




Contents lists available at ScienceDirect

## Atmospheric Environment

journal homepage: [www.elsevier.com/locate/atmosenv](http://www.elsevier.com/locate/atmosenv)

# Modeling the influence of biogenic volatile organic compound emissions on ozone concentration during summer season in the Kinki region of Japan

Hai Bao<sup>a</sup>, Kundan Lal Shrestha<sup>b,\*</sup>, Akira Kondo<sup>b</sup>, Akikazu Kaga<sup>b</sup>, Yoshio Inoue<sup>b</sup>

<sup>a</sup> Chemistry and Environment Science College, Inner Mongolia Normal University, Hohhot 010022, China

<sup>b</sup> Division of Sustainable Energy and Environmental Engineering, Graduate School of Engineering, Osaka University, Yamadaoka 2-1, Suita, Osaka 565-0871, Japan

## ARTICLE INFO

## Article history:

Received 26 May 2009

Received in revised form

13 October 2009

Accepted 14 October 2009

## Keywords:

Biogenic volatile organic compound

Ozone

MM5

CMAQ

Growth chamber

## ABSTRACT

Tropospheric ozone adversely affects human health and vegetation, and biogenic volatile organic compound (BVOC) emission has potential to influence ozone concentration in summer season. In this research, the standard emissions of isoprene and monoterpene from the vegetation of the Kinki region of Japan, estimated from growth chamber experiments, were converted into hourly emissions for July 2002 using the temperature and light intensity data obtained from results of MM5 meteorological model. To investigate the effect of BVOC emissions on ozone production, two ozone simulations for one-month period of July 2002 were carried out. In one simulation, hourly BVOC emissions were included (BIO), while in the other one, BVOC emissions were not considered (NOBIO). The quantitative analyses of the ozone results clearly indicate that the use of spatio-temporally varying BVOC emission improves the prediction of ozone concentration. The hourly differences of monthly-averaged ozone concentrations between BIO and NOBIO had the maximum value of 6 ppb at 1400 JST. The explicit difference appeared in urban area, though the place where the maximum difference occurred changed with time. Overall, BVOC emissions from the forest vegetation strongly affected the ozone generation in the urban area.

© 2009 Elsevier Ltd. All rights reserved.

## 1. Introduction

Photochemical oxidants cause a lot of damage to humans and vegetation. The increase in precursor emissions (oxides of nitrogen and volatile organic compounds) of ozone can significantly increase the ozone pollution (Emberson et al., 2001). It is well known that biogenic volatile organic compound (BVOC) emission increases with the rise in temperature and that BVOC plays an important role in the generation of ozone (Chameides et al., 1988). Though the impact of biogenic emission on ozone pollution is mainly observed in rural and suburban sites (Tsigaridis and Kanakidou, 2002), it can also be significant in urban region (Chameides et al., 1988; Solmon et al., 2004).

Vogel et al. (1995) used a non-hydrostatic mesoscale model coupled with a transport and diffusion model and the gas phase mechanism RADM2 to study the influence of BVOC emission on the ozone concentration during episodes of high air temperatures in the state of Baden-Württemberg, Germany. They found that simulations without using biogenic VOC emissions show a maximum difference in the ozone concentration of 18 ppb, while the maximum ozone

values are of the order of 100 ppb. They concluded that biogenic VOC emissions play an important role when high temperatures are present in Baden-Württemberg. Solmon et al. (2004) used Meso-NH–C mesoscale atmospheric chemistry model to study summertime biogenic emission impacts on regional ozone formation in Paris and northern France. They found that, when biogenic emission was included in the simulation, the simulated surface ozone concentration reached 18–30% in Paris. They also found improvement in simulated ozone concentrations at some observation stations in the urban and rural areas after including biogenic emissions.

In Japan, the standard for the photochemical oxidant was formulated in 1970, and due to its effectiveness, the concentration of photochemical oxidant decreased until 1990. However, recently the concentration of photochemical oxidant has been gradually increasing in Japan. One of its causes is the increase of the background ozone concentration due to transboundary transport (Akimoto, 2003). Furthermore, temperature increase due to global warming, urban heat island and the increase of ultraviolet rays (Wakamatsu et al., 1996) are also considered as some of its major causes.

Izuta (2002) has pointed out that, though the western countries have used AOT40 (Accumulated dose over a threshold of 40 ppb) as a critical level of ozone for the preservation of crops from ozone, Japan has yet to come up with such criteria of its own. BVOC

\* Corresponding author. Tel./fax: +81 (0) 6 68797670.

E-mail address: [kundan@ea.see.eng.osaka-u.ac.jp](mailto:kundan@ea.see.eng.osaka-u.ac.jp) (K.L. Shrestha).

emission from the indigenous plants of Japan has not been thoroughly investigated yet.

In this study, the rates of BVOC emission from the major plants of Japan were obtained from the growth chamber experiments, the total emission of BVOC in the Kinki region (Domain-2 in Fig. 1) was estimated, and the impacts of ozone generation due to the BVOC emission were assessed by MM5 (Grell et al., 1994; Dudhia et al., 2005) – CMAQ (Community Multiscale Air Quality) (Byun and Ching, 1999) modeling system.

## 2. Experiments and methods

### 2.1. Estimation of standard BVOC emission

Bao et al. (2008) conducted growth chamber experiments to estimate the standard emission rates of isoprene and monoterpene in the Kinki region. In these experiments, three coniferous trees (*Cryptomeria japonica*, *Chamaecyparis obtusa* and *Pinus densiflora*), six broadleaf trees (*Quercus serrata*, *Quercus crispula*, *Fagus crenata*, *Quercus acutissima* Carruthers, *Quercus glauca* and *Quercus myrsinaefolia*), and Asian rice (*Oryza sativa*) were selected. These three coniferous trees and six broadleaf trees occupied 59.8% and 18.2% respectively of the forest area in the Kinki region (Fig. 1). Similarly, paddy fields occupied 22% of the total area of the Kinki region. The plants under investigation were 3- to 5-year-old saplings that were planted in 10-L plastic pots. They were grown in open air and regularly watered and fertilized during the growing season to provide optimal growth conditions. Since a large portion of the area under research is covered by paddy fields, it is also important to measure the BVOC emissions of rice (*O. sativa*). Saplings of *O. sativa* were planted in 10-L plastic pots in spring and grown in open air until autumn. Standard emissions were measured by using a growth chamber, in which temperature and light intensity can be

manually set. Ten plants of each species were grown outside and individually transferred 24 h before the experiments to an 8800-L closed growth chamber. Attention was focused on minimizing physical damage to the plants. Air inside the growth chamber was hourly collected by using a 200 mg Tenax-TA adsorbent tube (Supelco, mesh 60/80) and a vacuum pump (GL Science SP208-1000Dual) with a flow rate of 100 ml min<sup>-1</sup>. For measuring the BVOC emissions from *C. japonica*, *C. obtusa*, *P. densiflora*, and *O. sativa*, air samples of 6 L were collected at every 1 h since the concentration of BVOC from these species are lower than deciduous broadleaf trees (air samples of 1 L). The photon flux density in the photosynthetically active wavelength range was measured using a photometer (LI-1600 LI-COR). The trapped compounds in the adsorbent tubes were thermally desorbed at 280 °C by Thermal Desorber (Perkin Elmer ATD-50) connected to GC/MS (Shimadzu GC/MS-QP2010), in which isoprene,  $\alpha$ -pinene,  $\beta$ -pinene, myrcene,  $\alpha$ -phellandrene,  $\alpha$ -terpinene, p-cymene, limonene,  $\gamma$ -terpinene and terpinolene were analyzed. The separation of BVOC was performed by a capillary column (30 m  $\times$  250  $\mu$ m  $\times$  0.25  $\mu$ m, J&W Scientific). The carrier gas was helium. The temperature was kept at 35 °C for 2 min, then raised to 70 °C at the rate of 20 °C min<sup>-1</sup>, and then kept at 70 °C for 10 min and finally raised to 280 °C at the rate of 20 °C min<sup>-1</sup>. The identification of BVOC was based on the GC peak retention time of reference standards. Samples were analyzed using the selective ion mode (SIM). The calibration factor for BVOC used for calculation of concentrations was checked periodically throughout the analysis (Bao et al., 2008).

In the growth chamber experiments, temperature was set according to the typical diurnal variation in Osaka City and photosynthetically active radiation (PAR) was set at 335 mmol m<sup>-2</sup> s<sup>-1</sup> or 1000 mmol m<sup>-2</sup> s<sup>-1</sup> from 0600 JST to 1800 JST. The BVOC emissions from the ten plant species at several conditions were converted to the standard condition (30 °C, PAR: 1000  $\mu$ mol m<sup>-2</sup> s<sup>-1</sup>) by using the

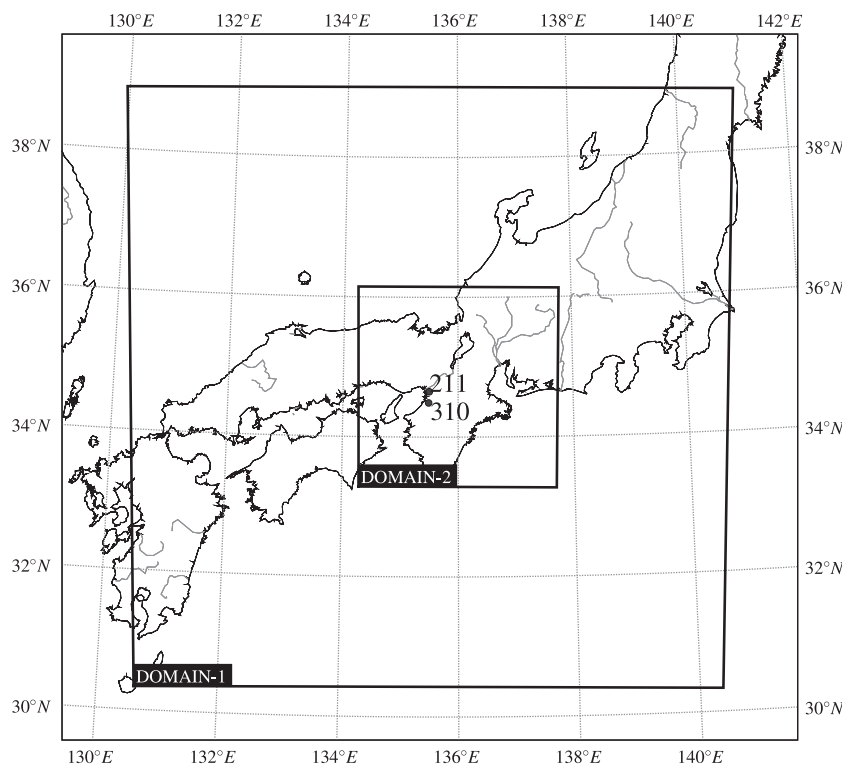


Fig. 1. Domains used for simulation. Domain-1 is 9-km grid structure and Domain-2 has 3-km grid structure. 211 and 310 stations are Imamiya Junior High School and Momoyamadai respectively.

**Table 1**  
Monoterpene emissions from coniferous trees at standard condition.

Compound	Monoterpene emission ( $\mu\text{g g}_{\text{dw}}^{-1} \text{h}^{-1}$ )			
	<i>C. japonica</i>	<i>C. obtusa</i>	<i>P. densiflora</i>	<i>O. sativa</i>
$\alpha$ -Pinene	1.30	1.89	5.33	0.24
$\beta$ -Pinene	0.06	0.22	0.84	0.02
Myrcene	0.32	0.35	1.79	0.03
$\alpha$ -Phellandrene	0.20	0.13	0.87	ND
$\alpha$ -Terpinene	0.15	0.13	0.23	ND
p-Cymene	0.10	0.28	0.14	0.03
Limonene	0.40	ND	0.82	0.08
$\gamma$ -Terpinene	0.21	0.49	ND	ND
Terpinolene	0.08	ND	0.27	ND
Total	2.81	3.48	10.28	0.40

All emissions have been normalized at 30 °C and PAR: 1000  $\mu\text{mol m}^{-2} \text{s}^{-1}$  using the algorithm by Guenther et al. (1993). ND means not detected.

Guenther equation (Guenther et al., 1993) and Tingey equation (Tingey et al., 1980). In order to assess the biomass of the enclosed plants, the dry weight of individual leaves was determined after drying the plant materials for 48 h at 105 °C. Using the mass of the dry leaves and the experimental data, BVOC emissions rates at standard condition were scaled per gram biomass ( $\mu\text{g g}_{\text{dw}}^{-1} \text{h}^{-1}$ ). Large amounts of  $\alpha$ -pinene and  $\beta$ -pinene were detected from *C. japonica*, *C. obtusa* and *P. densiflora*. Previously, *O. sativa* had not been reported to emit BVOC, but Bao et al. (2008) detected five kinds of monoterpenes from them. Though the amount of emission from *O. sativa* is small, it can contribute significantly to the overall emission because vast areas of Japan are occupied by paddy fields. Table 1 shows the monoterpenes emission at standard conditions. Table 2 shows isoprene emission at standard conditions from six deciduous broadleaf trees, which are commonly found in Japan. A large amount of isoprene was detected from *Q. serrata*.

The emissions of isoprene and monoterpene at the standard conditions in the Kinki region were estimated by using the forest database containing the data of dominant species of plant, occupied area, plant age, biomass and so on. This forest database was constructed by combining forest data from several prefecture offices of Kinki region (Osaka, Kyoto, Shiga, Hyogo, Nara, Mie, Wakayama, Fukui, Tottori, Okayama, Kagawa, and Tokushima) at 1-km grid resolution. Using the forest database, BVOC emissions potential maps were created. All the leaves were expected to receive the same amount of light. However, isoprene emissions may be slightly overestimated because isoprene emission is dependent on light intensity and our results do not consider the fact that there may be some leaves in the shade. The isoprene emission map is important and useful for the Kinki region considering that widely used inventories like MEGAN (Guenther et al., 2006) do not use explicit tree inventories and actual emission measurement for this region. MEGAN estimates of isoprene are based on classification according to ecoregions for regions without detailed forest database. MEGAN also assigns global average emission values for the regions without actual measurements of emissions.

**Table 2**  
Isoprene emissions from broadleaf trees at standard condition.

Plant name	Isoprene emission ( $\mu\text{g g}_{\text{dw}}^{-1} \text{h}^{-1}$ )
<i>Q. serrata</i>	153.06
<i>Q. crispula</i>	26.04
<i>F. crenata</i>	0.79
<i>Q. acutissima</i> Carruthers	0.18
<i>Q. glauca</i>	0.04
<i>Q. myrsinaefolia</i>	0.03

All emissions have been normalized at 30 °C and PAR: 1000  $\mu\text{mol m}^{-2} \text{s}^{-1}$  using the algorithm by Guenther et al. (1993).

In a particular region or ecosystem, there may be many tree species but only some of these may be producing major portion of the BVOC emissions. For example, total European isoprene emission is mainly dominated by *Quercus. petraea* and *Quercus. robur*, but if we investigate smaller regions, the dominant species for isoprene emission can vary from region to region (Simpson et al., 1999). In another case, enclosure experiments in a continental ecosystem in the U.S. showed that isoprene emission was dominated by a single oak species (Helmig et al., 1999). In the Kinki region (47,000 km<sup>2</sup>) investigated in this research, 425.7 ton h<sup>-1</sup> of isoprene were emitted. Deciduous biomass of Kinki region was 1.7 times larger than the broadleaf biomass but *Q. serrata* emitted a relatively large amount of isoprene emission, which contributed to 60% of the total isoprene emission. So the emissions of isoprene (Fig. 2) were extremely larger than the emissions of monoterpene (Fig. 3). The emission rate is high where *Q. serrata* is dominant in the region since *Q. serrata* emits large amount of isoprene. Since *Q. serrata* is exclusively found in Japan and some East Asian regions, its biogenic emissions cannot be compared with other parts of the world. The typically regional nature of *Q. serrata* and the abundance of its isoprene emission in Japan demonstrates the importance of the measurement and examination of its biogenic emissions in Japan. In the Kinki region, 60 ton h<sup>-1</sup> of monoterpenes were emitted. The emission rate of monoterpene is high where there are lots of coniferous trees, such as *C. japonica*, *C. obtusa*, and *P. densiflora*.

## 2.2. MM5 simulation

The final version (3.7) of MM5 was used without any four-dimensional data assimilation (FDDA). The simple ice scheme was used for the microphysics option. Dudhia's longwave and short-wave radiation scheme, Grell's cumulus parameterization scheme and Medium-Range Forecast (MRF) PBL scheme with multi-layer soil model were used.

The Grid Point Value–MesoScale Model (GPV–MSM) data from the Japan Meteorological Agency (JMA, <http://www.jma.go.jp/jma/index.html>) were used to initialize and force MM5. GPV–MSM data are available for the Japan region and have a high horizontal resolution of 10 km  $\times$  10 km.

The model region is shown in Fig. 1. Domain-1 has the resolution of 9 km and includes almost whole of Japan. Domain-2, having the resolution of 3 km and including the entire Kinki region, is nested inside Domain-1. Both Domain-1 and Domain-2 have 118  $\times$  118 horizontal grid cells and 23 vertical sigma-p layers.

The one-month time period of July 2002 was selected for summertime simulation. The meteorological output from MM5 were post-processed and used as meteorological input to drive the CMAQ model for ozone simulation (subsection 2.4). Moreover, the near-surface air temperature and incident solar radiation obtained from MM5 were used to calculate hourly BVOC emission (subsection 2.3).

## 2.3. Estimation of hourly BVOC emission

Hourly emissions of isoprene vary according to the hourly variations of temperature and light intensity (Tingey et al., 1980; Guenther et al., 1991, 1995). The standard emissions obtained from growth chamber (subsection 2.1) were converted into hourly emissions of July 2002 using the temperature and light intensity, which were calculated by using MM5 output. Guenther equation for isoprene and Tingey equation for monoterpene were used to calculate the emissions variation due to temperature and light intensity. The equation of isoprene emission is expressed by

$$E_{\text{iso}} = EF_{\text{iso}} C_T C_L \quad (1)$$

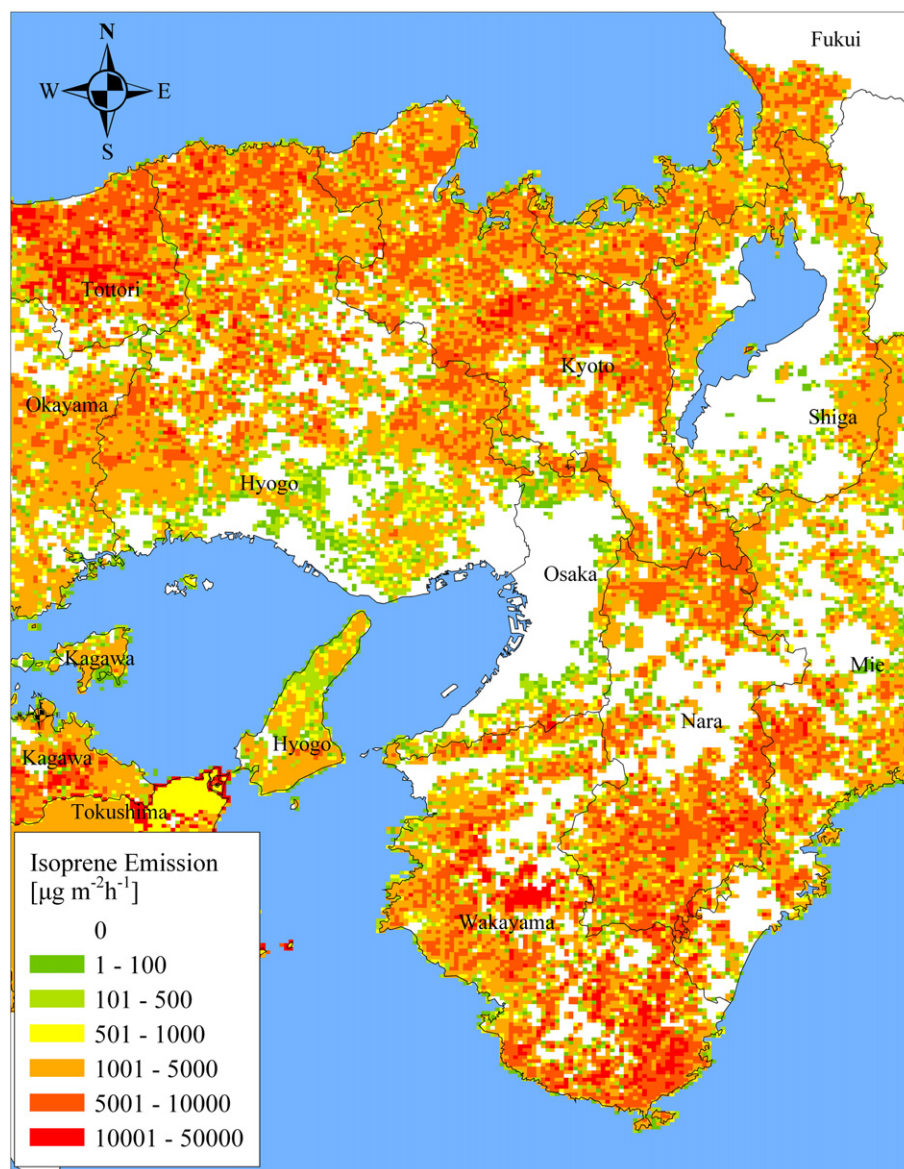


Fig. 2. Standard emissions of isoprene in the Kinki region.

where  $EF_{iso}$  ( $\mu\text{g g}_{\text{dw}}^{-1} \text{h}^{-1}$ ) is the isoprene emission rate at standard conditions.  $C_T$  is the correction factor due to temperature and  $C_L$  is the correction factor due to PAR.  $C_T$  and  $C_L$  are defined as

$$C_T = \frac{\exp\left(\frac{C_{T1}(T - T_S)}{RTT_S}\right)}{1 + \exp\left(\frac{C_{T2}(T - T_M)}{RT_S T}\right)} \quad (2)$$

$$C_L = \frac{\alpha C_{L1} L}{\sqrt{1 + \alpha^2 L^2}} \quad (3)$$

where  $\alpha$  ( $0.0027$ ),  $C_{L1}$  ( $1.066$ ),  $C_{T1}$  ( $95,000 \text{ J mol}^{-1}$ ),  $C_{T2}$  ( $230,000 \text{ J mol}^{-1}$ ) and  $T_m$  ( $314 \text{ K}$ ) are empirical coefficients,  $L$  ( $\mu\text{mol m}^{-2} \text{s}^{-1}$ ) is the PAR flux,  $T_S$  ( $303 \text{ K}$ ) is the standard reference temperature,  $R$  ( $8.314 \text{ J K}^{-1} \text{ mol}^{-1}$ ) is the ideal gas constant and  $T$  ( $\text{K}$ ) is the foliar biomass temperature. PAR flux is calculated as

$$L = 4.6 CF SW_{\downarrow} \quad (4)$$

where  $4.6$  ( $\mu\text{mol J}^{-1}$ ) is multiplier used for converting energy unit to quantum unit,  $CF$  is conversion factor ( $0.5$ ) and  $SW_{\downarrow}$  ( $\text{W m}^{-2}$ ) is downward shortwave radiation obtained from MM5 simulation.

The equation of monoterpene emission is expressed by

$$E_{\text{mono}} = EF_{\text{mono}} \exp(\beta(T - T_S)) \quad (5)$$

where  $EF_{\text{mono}}$  ( $\mu\text{g g}_{\text{dw}}^{-1} \text{h}^{-1}$ ) is the monoterpene emission rate at standard temperature, and  $\beta$  is an empirical coefficient ranging between  $0.057$  and  $0.144 \text{ K}^{-1}$ .  $\beta$  can vary according to chemical species and environmental conditions.  $0.09 \text{ K}^{-1}$  is a reasonable estimate for monoterpene emissions of most plants. In this research, the effect of solar radiation on monoterpene emission is not considered. Moreover, the reduction in BVOC emissions from coniferous trees due to ozone exposure is also not considered.

#### 2.4. Ozone simulation using CMAQ model

CMAQ model is a third generation air quality model that can be used to study tropospheric ozone, particulate matter and other air

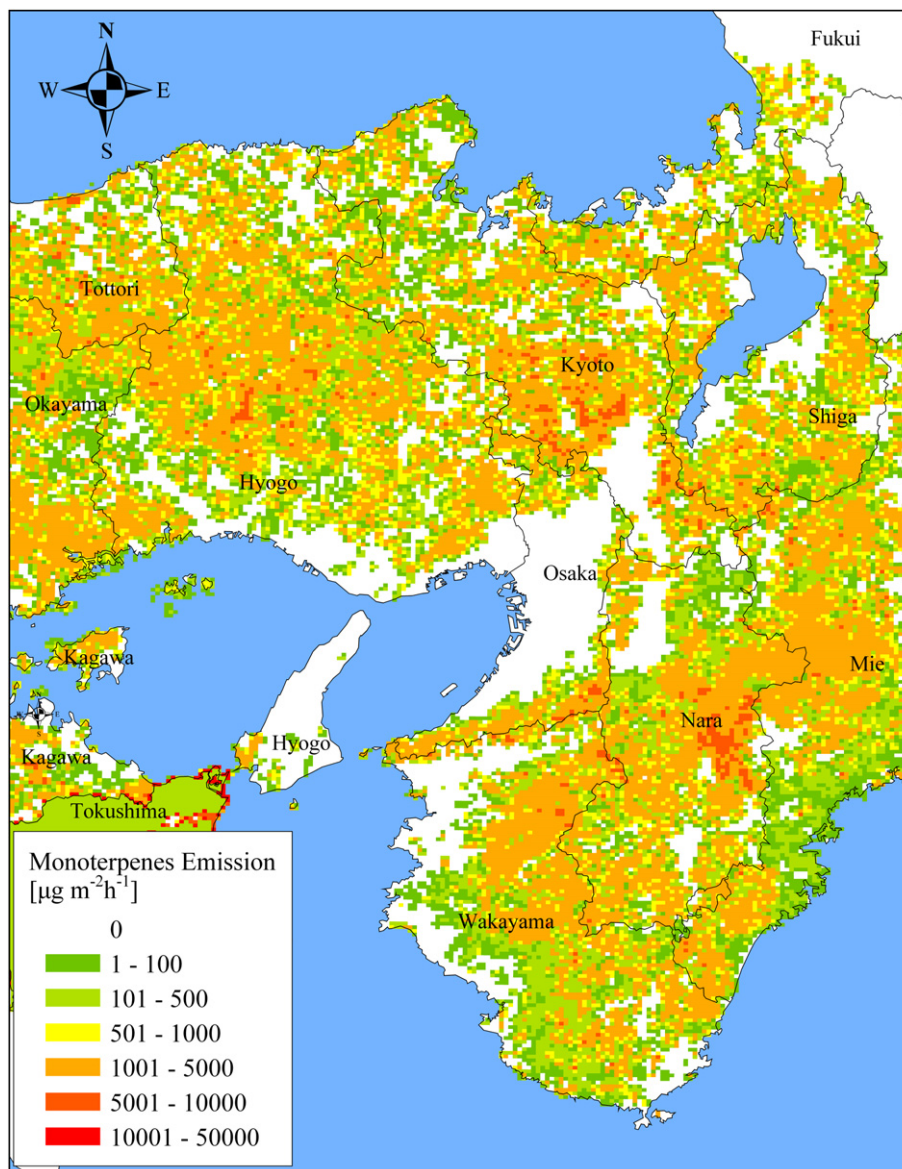


Fig. 3. Standard emissions of monoterpene in the Kinki region.

pollution issues at regional and urban scales (Byun and Ching, 1999). The meteorological fields needed for CMAQ modeling is generated by MM5. CMAQ was configured with a chemical mechanism called Statewide Air Pollution Research Center (SAPRC-99) mechanism, which provides a detailed mechanism for the gas-phase atmospheric reactions of volatile organic compounds (VOCs) and oxides of nitrogen (NO<sub>x</sub>) in urban and regional atmospheres. For the simulation domains in CMAQ model, the boundary was trimmed in both the 9-km and 3-km domains to minimize the boundary effects from the meteorological models. Therefore, Domain-1 and Domain-2 have 105 × 105 horizontal grid cells.

The mobile emission source data needed for CMAQ modeling was obtained from Japan Clean Air Program (JCAP) of Japan ([http://www.pecj.or.jp/japanese/jcap/airmodel/index\\_airmodel.html](http://www.pecj.or.jp/japanese/jcap/airmodel/index_airmodel.html), in Japanese). The surface area data contains the stationary area source and mobile source emissions. This data also includes weekday and weekend mobile emission data. For other emission source data needed for CMAQ modeling, the national emission data with the spatial resolution of 0.125 degree by 0.0833 degree were used.

These emission data are provided as the hourly average data for the month of July and they are preprocessed by a separate program to convert them into hourly data needed as input in CMAQ model for the simulation period. The hourly BVOC emission data described in subsection 2.3 were used.

To investigate the effect of BVOC emissions on ozone production, two simulations for one-month period of July 2002 were carried out. One is the calculation with hourly BVOC emissions (BIO). Another is the calculation that assumes BVOC emissions to be zero (NOBIO). Then, ozone concentrations obtained from the CMAQ simulation were analyzed.

### 3. Results and discussion

#### 3.1. Temperature and solar radiation

The meteorological variables such as air temperature and solar radiation are important for accurate simulation of surface ozone. In the case of near-surface air temperature, MM5 simulated the

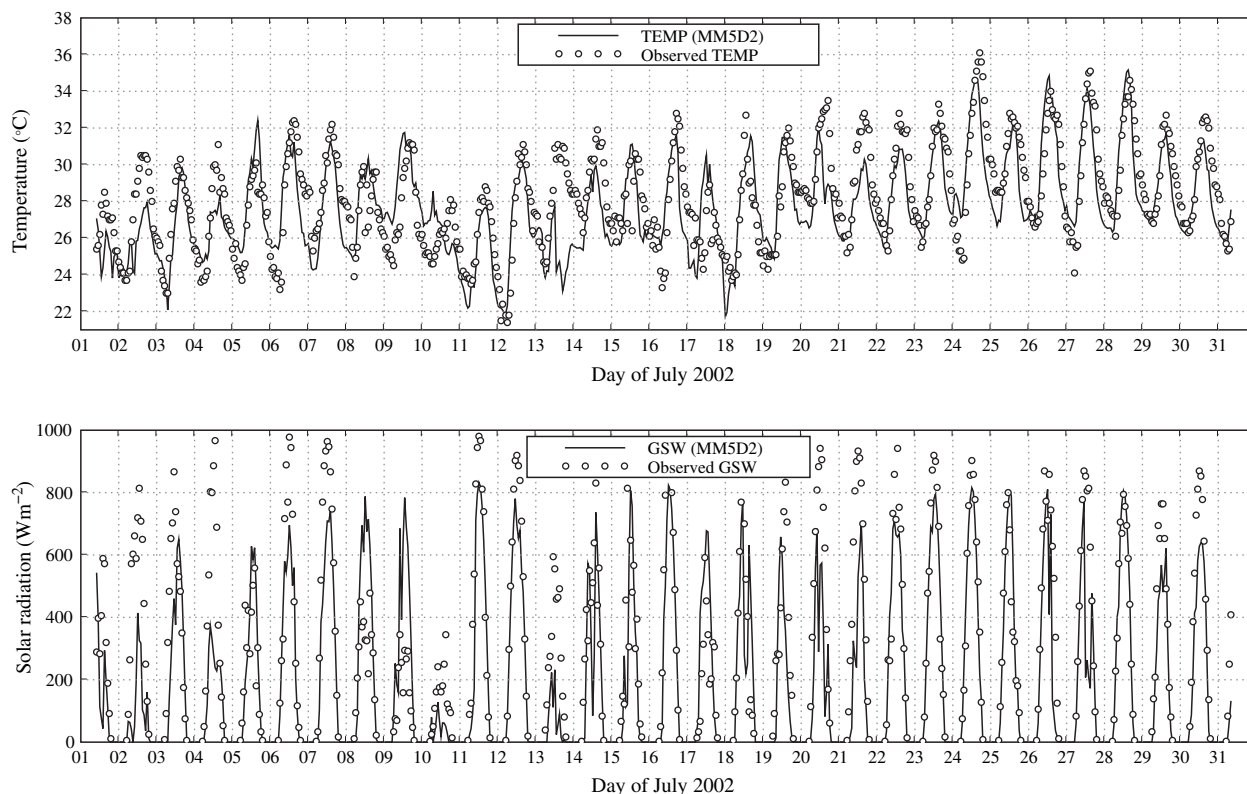


Fig. 4. Comparison of time series of air temperature and solar radiation at station no. 310 with observation data at the observation point nearest to the station.

diurnal variation with high correlation of 0.79 for hourly air temperature (Fig. 4). Low mean bias of  $-0.98$  K was obtained for near-surface air temperature. Though the rainy days on July 10 and 13 (not shown in figure) were well reproduced with corresponding low solar radiation values, MM5 predicted rain throughout the day of July 13 but the actual precipitation occurred in the morning time only. Therefore, large underpredictions of solar radiation and overprediction of precipitation on July 13 by MM5 may have partially contributed to underprediction of the diurnal pattern of air temperature.

For solar radiation from MM5, mean bias of  $-82.5$   $\text{W m}^{-2}$  and correlation coefficient of 0.69 were obtained when compared with observed data. Solar radiation is generally well predicted by MM5 with underpredictions in the peak values in most of the days of July 2002. On July 2 and 3, the solar radiation may have been underpredicted by MM5 due to overprediction of precipitation. Overall, MM5 simulated temperature and solar radiation with low mean bias and high correlation when compared with the observed data.

Near-surface air temperature and incident solar radiation data were used in the calculation of hourly BVOC emissions for the CMAQ simulation of ozone in the Kinki region. Moreover, the meteorological outputs of MM5 were used to drive the CMAQ model.

### 3.2. Hourly BVOC emission

The hourly isoprene and monoterpene emissions in the Kinki region (e.g., Fig. 5 for isoprene emission and Fig. 6 for monoterpene emission) were calculated for July 2002 using Eqs. (1) and (5) respectively. The hourly BVOC emissions were calculated for 3-km grid structure of Domain-2 in Fig. 1. Kinki region's area-averaged total hourly variations of isoprene and monoterpene in July 2002

are shown in Fig. 7. As there were many cloudy or rainy days in the first half of this month, the emissions were relatively low. Diurnal profiles of isoprene and monoterpene emissions, averaged over one month of July 2002 clearly indicate the diurnal characteristics of isoprene and monoterpene emissions in summer season (Fig. 8). In the daytime, isoprene and monoterpene emissions were almost same, but only monoterpene emissions were emitted in the nighttime.

### 3.3. Impact of BVOCs on ozone concentration

#### 3.3.1. Comparison of ozone time series with observed data

The calculated ozone concentrations were compared at two observation stations (Imamiya Junior High School and Momoyamadai), where the relatively high concentrations were observed. Imamiya Junior High School (station no. 211) is located at the center of Osaka City and Momoyamadai (station no. 310) is located at the southern part of Osaka Prefecture (Fig. 1).

The high ozone concentrations were observed on 23, 24, 27, 28, 29 and 30 July, 2002 as shown in Fig. 9. These days had fair weather conditions, the temperature was relatively high and the solar radiation was strong. Consequently a lot of BVOCs were emitted from the forest area. The ozone concentrations of BIO became higher than NOBIO and reasonably reproduced the observed concentrations. For example, the peak observed ozone concentration and the peak ozone concentration of BIO and NOBIO at Momoyamadai (station no. 310) on 23 July were 122 ppb (exceeding the official ozone warning level of 120 ppb, and the highest ozone day in July 2002), 110 ppb and 84 ppb, respectively. In the case of Imamiya Junior High School (station no. 211), the peak observed ozone concentration and the peak ozone concentration of BIO and NOBIO on 23 July were 110 ppb, 90 ppb and 70 ppb,

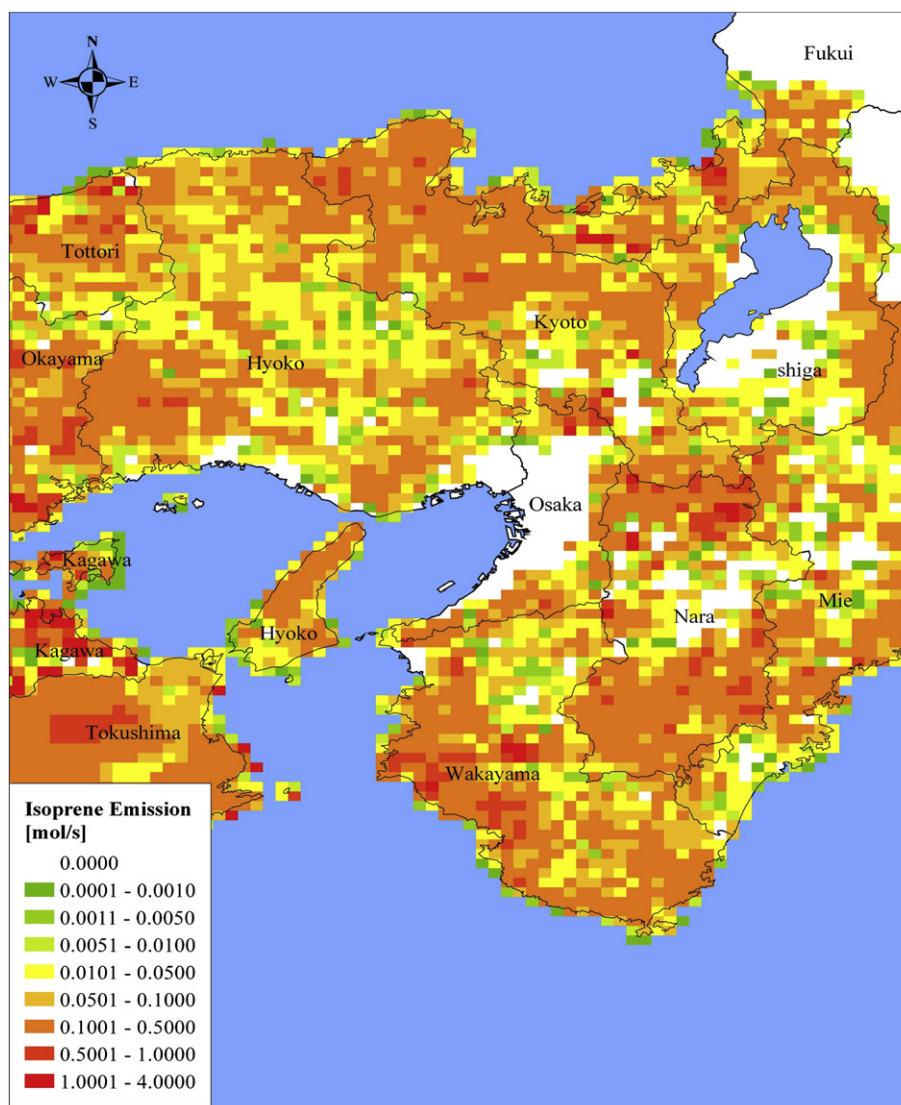


Fig. 5. Emissions of isoprene in Kinki region at 1400 JST in 23 July, 2002. The 3-km grids contain the emissions varying according to the meteorological conditions.

respectively. Hence, BVOC emissions increased the peak ozone concentration by 26 ppb and 20 ppb respectively at Momoyamadai and Imamiya Junior High School. Overall, the inclusion of BVOC emissions moved the simulated peak ozone concentrations closer to the observed values.

In the first half of July 2002, when BVOC emissions were rather small due to the cloudy days, the differences between the ozone concentration of BIO and NOBIO can't be seen. In the second half of July 2002 having strong solar radiation, high air temperature and low wind speed, the BIO time series at daytime gets closer to the observed time series than the NOBIO time series. On the other hand, cloudy day of July 4, rainy days of July 10 and 13, and windy days of July 25 and 26 do not have significant differences between BIO and NOBIO time series. Since BVOC emissions strongly depend upon the air temperature and light intensity, BVOC emissions increase during sunny and high-temperature days. But in cloudy and rainy days, the amount of BVOC emission lowers and consequently its effect on ozone concentration is usually not observed.

The statistical analyses of BIO and NOBIO cases (Table 3) were carried out for ozone concentrations greater than 40 ppb using

correlation coefficient ( $r$ ), mean bias (MB), mean normalized bias (MNB), normalized mean bias (NMB), and normalized mean bias factor (NMBF) (Yu et al. (2006)) shown respectively in Eqs. (6)–(10), where  $M_i$  and  $O_i$  are model-simulated and observation data at time and location  $i$  respectively,  $N$  is the number of pairs of data,  $\bar{M} = \frac{1}{N} \sum_{i=1}^N M_i$  and  $\bar{O} = \frac{1}{N} \sum_{i=1}^N O_i$ .

$$r = \frac{\left\{ \sum_{i=1}^N (M_i - \bar{M})(O_i - \bar{O}) \right\}}{\left\{ \sum_{i=1}^N (M_i - \bar{M})^2 \sum_{i=1}^N (O_i - \bar{O})^2 \right\}^{\frac{1}{2}}} \quad (6)$$

$$MB = \frac{1}{N} \sum_{i=1}^N (M_i - O_i) = \bar{M} - \bar{O} \quad (7)$$

$$MNB = \frac{1}{N} \sum_{i=1}^N \left( \frac{M_i}{O_i} - 1 \right) \quad (8)$$

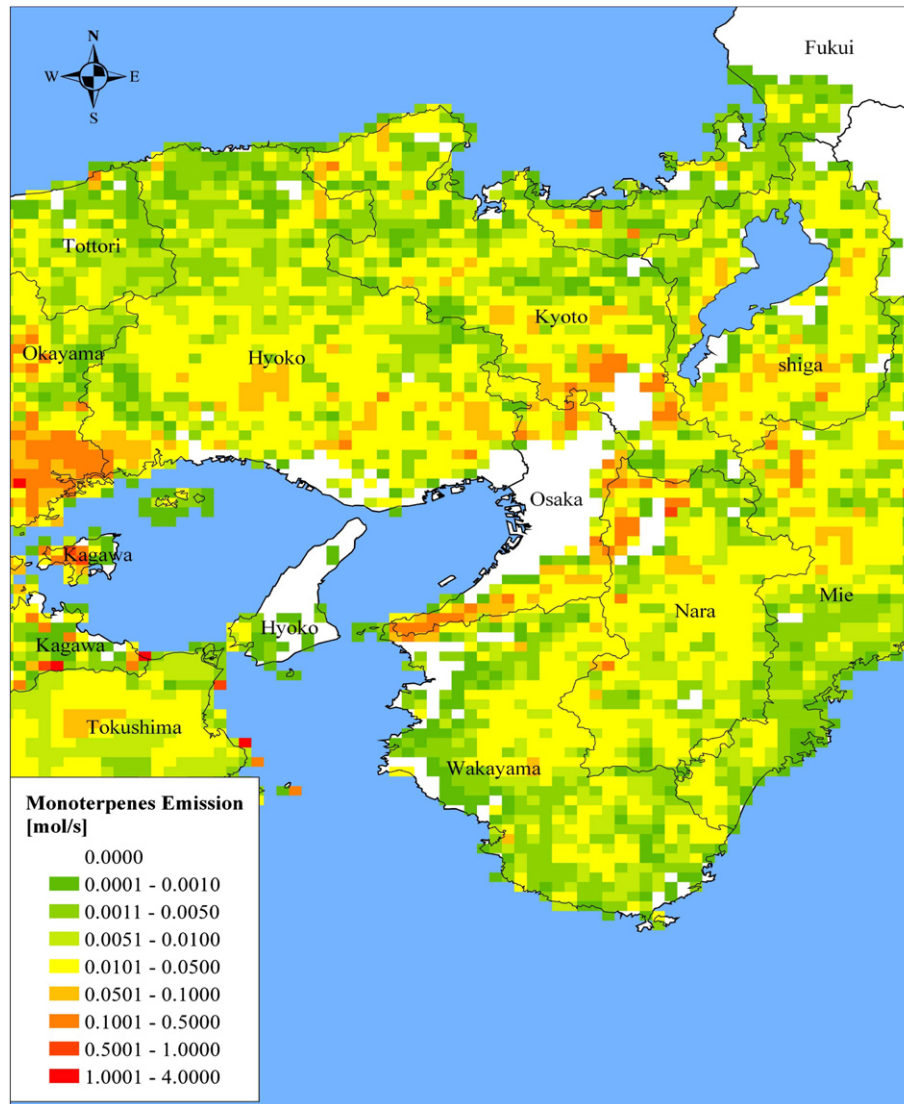


Fig. 6. Emissions of monoterpene in Kinki region at 1400 JST in 23 July, 2002. The 3-km grids contain the emissions varying according to the meteorological conditions.

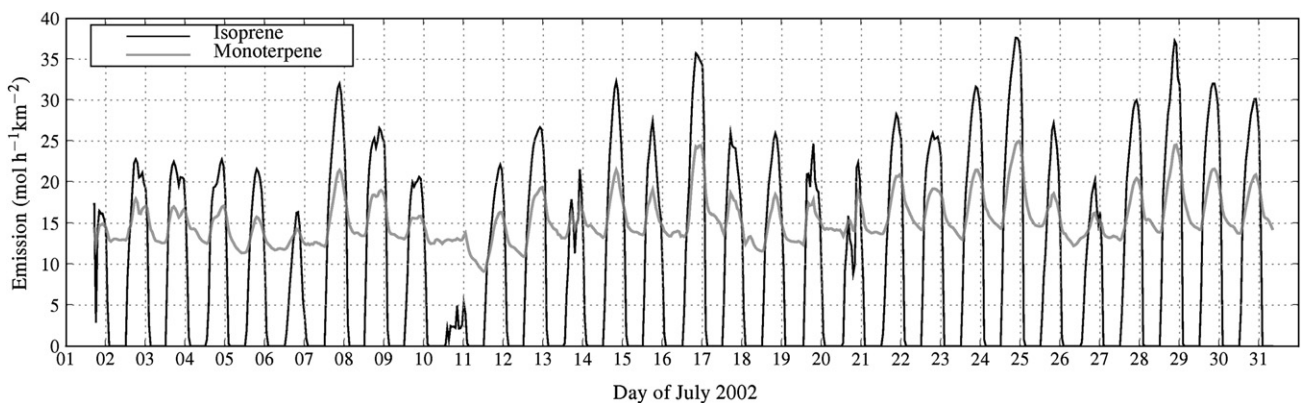


Fig. 7. Area-averaged hourly variations of isoprene and monoterpene emissions for the Kinki region.



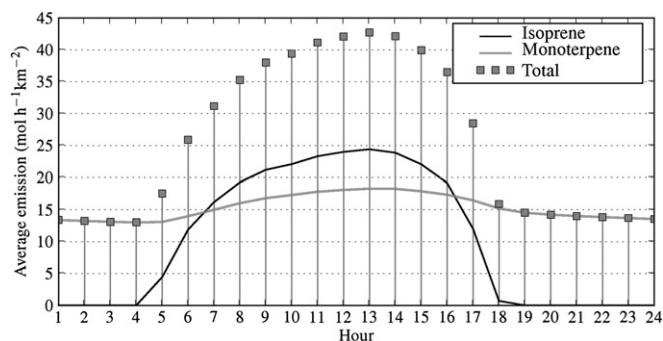


Fig. 8. Diurnal profile of isoprene and monoterpene emissions averaged over one-month period of July 2002 for the Kinki region.

$$\text{NMB} = \frac{\bar{M}}{\bar{O}} - 1 \quad (9)$$

$$\text{NMBF} = \begin{cases} \frac{\bar{M}}{\bar{O}} - 1 & \text{for } \bar{M} \geq \bar{O} \\ 1 - \frac{\bar{O}}{\bar{M}} & \text{for } \bar{M} < \bar{O} \end{cases} \quad (10)$$

The correlation coefficient of BIO improved to 0.41 from 0.31 ( $p < 0.05$ ) and the mean bias also improved to  $-0.81$  ppb from  $-6.05$  ( $p < 0.01$ ). Mean normalized bias (MNB), normalized mean bias (NMB) and normalized mean bias factor (NMBF), which are the evaluation index for the ozone recommended by US EPA, also improved. Thus the statistical results also suggest that a good

Table 3

Statistical results of BIO and NOBIO cases for ozone concentrations greater than 40 ppb.

Metrics	BIO	NOBIO
Correlation coefficient	0.41	0.37
Mean bias (MB)	$-0.81$	$-6.03$
Mean normalized bias (MNB)	0.03	$-0.06$
Normalized mean bias (NMB)	$-0.01$	$-0.10$
Normalized mean bias factor (NMBF)	$-0.01$	$-0.11$

representation of BVOC emissions is essential for better simulation of ozone concentrations.

### 3.3.2. Monthly-averaged diurnal variation of ozone

The monthly-averaged hourly differences of ozone concentrations between BIO and NOBIO were investigated. As the photochemical reaction doesn't occur at nighttime, ozone concentrations of BIO and NOBIO cases were almost same. From sunrise, the difference of ozone concentrations between the BIO and NOBIO cases appeared, and as the temperature gradually rose at daytime, this difference reached to 6 ppb at 1400 JST. Difference of ozone concentrations between the BIO and NOBIO cases was observed until 1800 JST. The monthly-averaged differences of ozone concentrations between the BIO and NOBIO cases from 1200 JST to 1700 JST are shown in Fig. 10.

The difference between the BIO and NOBIO cases at daytime appeared in urban area, though the place where the maximum difference occurred changed with time. In almost all hours the maximum difference emerged at the border of Osaka City where

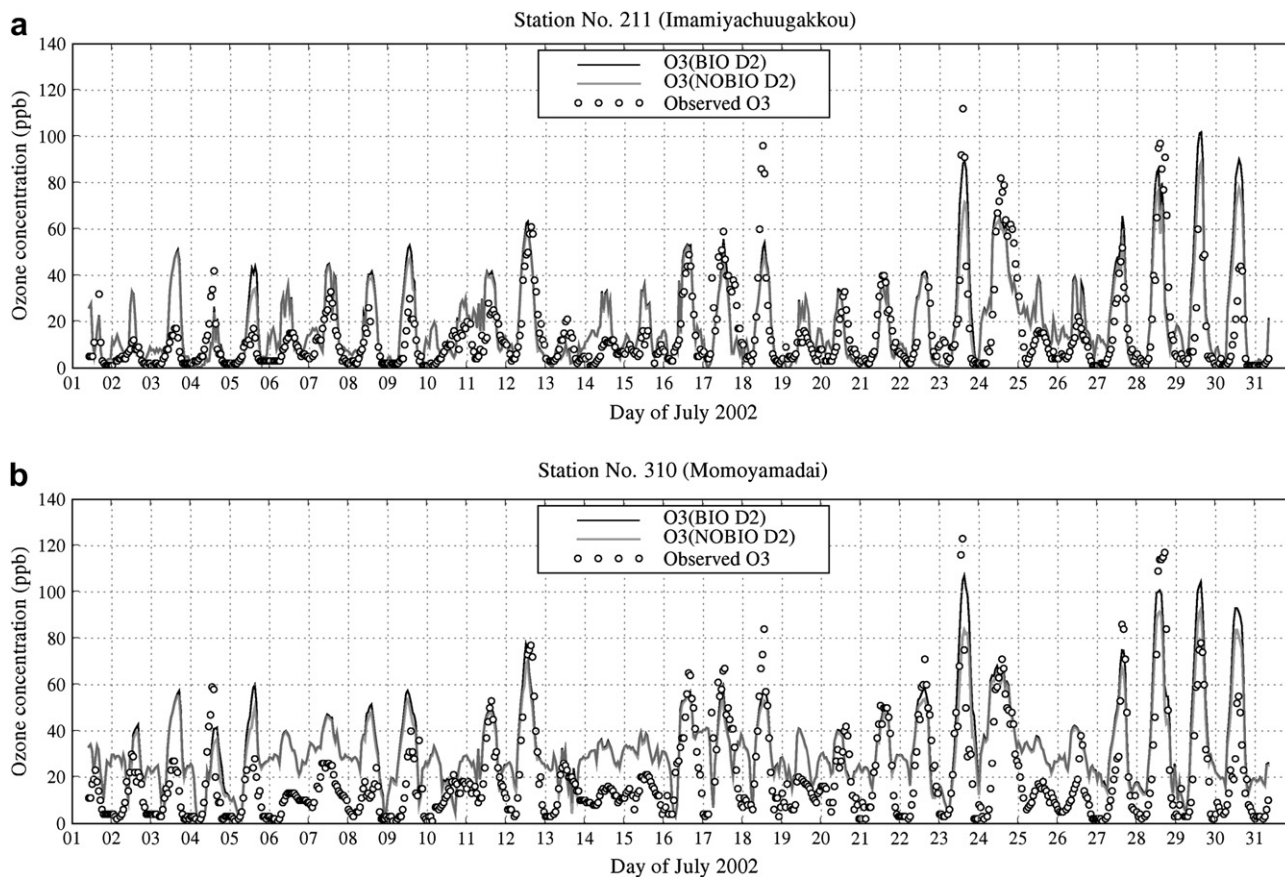
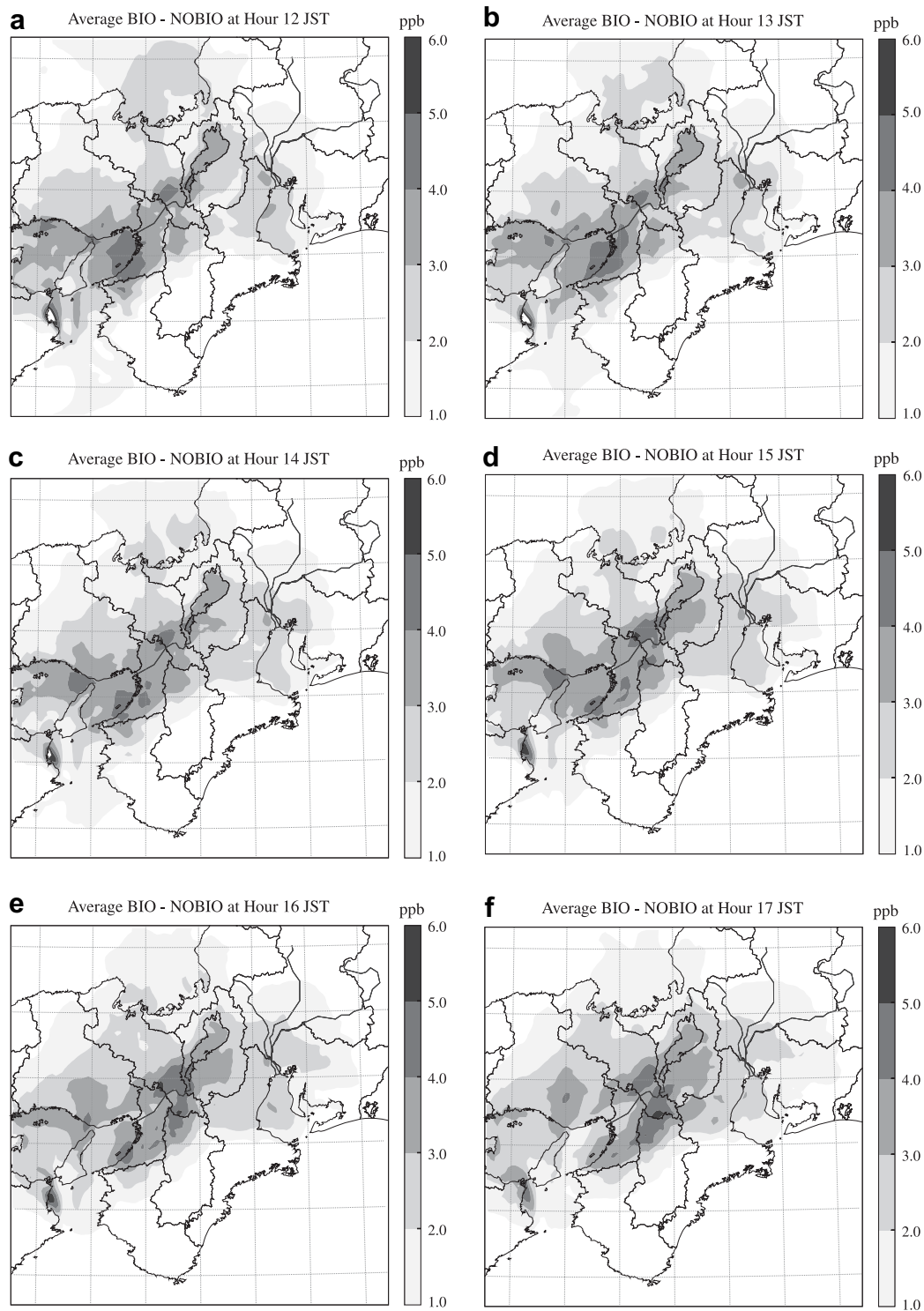


Fig. 9. Calculated and observed ozone concentration at Imamiya Junior High School and Momoyamadai.



**Fig. 10.** Hourly differences of monthly-averaged ozone concentrations between BIO and NOBIO cases.

a large amount of NO<sub>x</sub> gets emitted. Subsequently, due to the increase in the photochemical reaction between NO<sub>x</sub> and BVOC, ozone production increases. It was shown that the BVOCs emissions from the forest area strongly affected the ozone generation in the urban area. The inclusion of BVOCs from vegetation in ozone simulation produced a maximum of 6 ppb increase in monthly-averaged daytime ozone concentration, and hence, BVOCs have a significant impact on the production of tropospheric ozone. Thus,

the simulation and evaluation of ozone in urban area also needs a good consideration of BVOC emissions from vegetation.

BVOC estimates from this research likely have uncertainties that are associated with inherent measurement errors and modeling uncertainties. Since the biomass and forest coverage data are collected from various sources, some uncertainties due to this data limitation may be present. The actual shading effect on some portions of the biomass may also introduce some uncertainties in

the modeling. The representation of the dependence of isoprene and monoterpene emissions on temperature and light intensity also contributes to the model uncertainties. Moreover, some bias errors in the meteorological variables from the MM5 also affect BVOC modeling. In spite of these measurement and model uncertainties, high-resolution BVOC emission data generated and used for the ozone simulation in Kinki region of Japan has potential to improve the simulation and prediction of BVOCs and ozone in this region.

#### 4. Conclusion

In this research, standard emission rates of BVOCs from the vegetation of Kinki region of Japan and meteorological output from MM5 were used to calculate gridded hourly BVOC emissions for 9-km and 3-km grid structures covering whole Japan and Kinki region respectively. Subsequently, hourly ozone concentration was simulated by CMAQ model using the MM5 output variables and the hourly BVOC emissions.

One-month ozone simulation for July 2002 was carried out using CMAQ model to observe the impact of BVOC emissions from the vegetation of Kinki region on ozone concentration in the summer season. Two cases of ozone simulation were conducted. In the first case (BIO), the effects of BVOCs were taken into consideration, while in the second case (NOBIO) such effects were neglected. Peak ozone concentration increased by 26 ppb and 20 ppb respectively at Momoyamadai and Imamiya Junior High School when BVOC emissions were taken into account. Thus the addition of BVOC emissions in the CMAQ simulation brought the simulated peak ozone concentrations nearer to the observed values. Similarly, the Kinki region experienced a maximum of 6 ppb increase in monthly-averaged daytime ozone concentration due to the effect of BVOC emission on ozone.

The coniferous trees, broadleaf trees and paddy fields in the Kinki region contributed significantly to the BVOC emissions during the summer season of 2002. Consequently, these BVOC emissions clearly affected the ozone production in the urban area of Osaka City and its surrounding region by increasing the ozone concentration. Also, the quantitative analysis of ozone concentrations confirmed the significance of using BVOC emissions from vegetation in ozone simulation. The detrimental effect of tropospheric ozone on the urban environment and its surrounding region is notably influenced and enhanced by the BVOC emissions from the vegetation. Hence, accurate representation of spatially and temporally varying BVOC emissions in air quality models is needed to improve ozone predictions in regions having considerable amount of BVOC emissions from vegetation.

#### Acknowledgments

We are grateful to Japan Clean Air Program (JCAP) of Japan Petroleum Energy Center (JPEC), Tokyo, Japan for providing the Japanese emission data used in this research.

#### References

- Akimoto, H., 2003. Global air quality and pollution. *Science* 302 (5651), 1716–1719.
- Bao, H., Kondo, A., Kaga, A., Tada, M., Sakaguti, K., Inoue, Y., Shimoda, Y., Narumi, D., Machimura, T., 2008. Biogenic volatile organic compound emission potential of forests and paddy fields in the Kinki region of Japan. *Environmental Research* 106 (2), 156–169.
- Byun, D.W., Ching, J.K.S. (Eds.), 1999. *Science Algorithms of the EPA Models-3 Community Multiscale Air Quality Model (CMAQ) Modeling System*. US Environmental Protection Agency, Office of Research and Development, Washington, DC.
- Chameides, W., Lindsay, R., Richardson, J., Kiang, C., 1988. The role of biogenic hydrocarbons in urban photochemical smog: Atlanta as a case study. *Science* 241 (4872), 1473–1475.
- Dudhia, J., Gill, D., Manning, K., Wang, W., Bruyere, C., 2005. *PSU/NCAR Mesoscale Modeling System Tutorial Class Notes and Users' Guide: MM5 Modeling System Version 3*.
- Emberson, L., Ashmore, M., Murray, F., Kuylentierna, J., Percy, K., Izuta, T., Zheng, Y., Shimizu, H., Sheu, B., Liu, C., Agrawal, M., Wahid, A., Abdel-Latif, N., van Tienhoven, M., de Bauer, L., Domingos, M., 2001. Impacts of air pollutants on vegetation in developing countries. *Water, Air, & Soil Pollution* 130 (1), 107–118.
- Grell, G.A., Dudhia, J., Stauffer, D.R., 1994. A description of the fifth-generation Penn State/NCAR mesoscale model (MM5). NCAR Technical Note NCAR/TN-398+STR.
- Guenther, A., Hewitt, C.N., Erickson, D., Fall, R., Geron, C., Graedel, T., Harley, P., Klinger, L., Lerdau, M., Mckay, W.A., Pierce, T., Scholes, B., Steinbrecher, R., Tallamraju, R., Taylor, J., Zimmerman, P., 1995. A global model of natural volatile organic compound emissions. *Journal of Geophysical Research* 100 (D5), 8873–8892.
- Guenther, A., Karl, T., Harley, P., Wiedinmyer, C., Palmer, P.I., Geron, C., 2006. Estimates of global terrestrial isoprene emissions using MEGAN (Model of Emissions of Gases and Aerosols from Nature). *Atmospheric Chemistry and Physics* 6 (11), 3181–3210.
- Guenther, A., Zimmerman, P., Harley, P., Monson, R., Fall, R., 1993. Isoprene and monoterpene emission rate variability: model evaluations and sensitivity analyses. *Journal of Geophysical Research* 98 (D7), 12609–12617.
- Guenther, A.B., Monson, R.K., Fall, R., 1991. Isoprene and monoterpene emission rate variability: observations with eucalyptus and emission rate algorithm development. *Journal of Geophysical Research* 96 (D6), 10799–10808.
- Helmig, D., Klinger, L.F., Guenther, A., Vierling, L., Geron, C., Zimmerman, P., 1999. Biogenic volatile organic compound emissions (BVOCs) II. Landscape flux potentials from three continental sites in the U.S. *Chemosphere* 38 (9), 2189–2204.
- Izuta, T., 2002. Studies on the effects of ozone and acid deposition on Japanese crop plants and forest tree species. *Journal of Japan Society for Atmospheric Environment* 37 (2), 81–95 (in Japanese).
- Simpson, D., Winiwarter, W., Börjesson, G., Cinderby, S., Ferreiro, A., Guenther, A., Hewitt, C.N., Janson, R., Khalil, M.A.K., Owen, S., Pierce, T.E., Puxbaum, H., Shearer, M., Skiba, U., Steinbrecher, R., Tarrasón, L., Öquist, M.G., 1999. Inventorying emissions from nature in Europe. *Journal of Geophysical Research* 104 (D7), 8113–8152.
- Solmon, F., Sarrat, C., Serça, D., Tulet, P., Rosset, R., 2004. Isoprene and monoterpenes biogenic emissions in France: modeling and impact during a regional pollution episode. *Atmospheric Environment* 38 (23), 3853–3865.
- Tingey, D.T., Manning, M., Grothaus, L.C., Burns, W.F., 1980. Influence of light and temperature on monoterpene emission rates from slash pine. *Plant Physiology* 65 (5), 797–801.
- Tsigaridis, K., Kanakidou, M., 2002. Importance of volatile organic compounds photochemistry over a forested area in central Greece. *Atmospheric Environment* 36 (19), 3137–3146.
- Vogel, B., Fiedler, F., Vogel, H., 1995. Influence of topography and biogenic volatile organic compounds emission in the state of Baden-Württemberg on ozone concentrations during episodes of high air temperatures. *Journal of Geophysical Research* 100 (D11), 22907–22928.
- Wakamatsu, S., Ohara, T., Uno, I., 1996. Recent trends in precursor concentrations and oxidant distributions in the Tokyo and Osaka areas. *Atmospheric Environment* 30 (5), 715–721.
- Yu, S., Eder, B., Dennis, R., Chu, S.-H., Schwartz, S.E., 2006. New unbiased symmetric metrics for evaluation of air quality models. *Atmospheric Science Letters* 7 (1), 26–34.